Original Article
Yonsei Med J 2021 Nov;62(11):1032-1041
https://doi.org/10.3349/ymj.2021.62.11.1032
Yonsei Medical Journal
YMJ
pISSN: 0513-5796 · eISSN: 1976-2437

Characterization of Ferric Chloride-Induced Arterial Thrombosis Model of Mice and the Role of Red Blood Cells in Thrombosis Acceleration

Yeseul Shim[1,2,3], Il Kwon[2], Youngseon Park[1,2,3], Heow Won Lee[2], Jayoung Kim[1], Young Dae Kim[1,2], Hyo Suk Nam[1,2], Sungha Park[2,4], and Ji Hoe Heo[1,2,3]

[1]Department of Neurology, Yonsei University College of Medicine, Seoul;
[2]Integrative Research Institute for Cerebrovascular and Cardiovascular Diseases, Yonsei University College of Medicine, Seoul;
[3]Department of Neurology, Graduate School of Medical Science, Brain Korea 21 Project, Yonsei University College of Medicine, Seoul;
[4]Division of Cardiology, Department of Internal Medicine, Yonsei University College of Medicine, Seoul, Korea.

Purpose: The ferric chloride ($FeCl_3$)-induced thrombosis model is widely used for thrombosis research. However, it lacks standardization with uncertainty in the exact mechanism of thrombosis. This study aimed to characterize thrombus formation in a mouse model.

Materials and Methods: We investigated thrombus formation and stability using various $FeCl_3$ concentrations (10%, 20%, 30%, 40%, and 50%, w/v) in carotid arteries of the Institute of Cancer Research (ICR) and C57BL/6N mice using the $FeCl_3$-induced thrombosis model. We also investigated thrombus histopathology using immunohistochemistry and electron microscopy.

Results: Higher $FeCl_3$ concentrations induced dose-dependent, faster, larger, and more stable thrombus formation in both strains of mice. However, the ICR mice showed better dose-responses in thrombus formation and stability compared to the C57BL/6N mice. Thrombi were fibrin- and platelet-rich without significant changes across $FeCl_3$ concentrations. However, the content of red blood cells (RBCs) increased with increasing $FeCl_3$ concentrations (p for trend <0.001) and inversely correlated with time to occlusion (r=-0.65, p<0.001). While platelets and fibrin were evenly distributed over the thrombus, RBCs were predominantly located near the $FeCl_3$ treatment area. Transmission electron microscopy showed that RBCs attached to and were surrounded by aggregates of degranulated platelets, suggesting their potential role in platelet activation.

Conclusion: Faster and larger thrombus formation is induced in a dose-dependent manner by a wide range of $FeCl_3$ concentrations, but the stable thrombus formation requires higher $FeCl_3$ concentrations. Mouse strain affects thrombus formation and stability. RBCs and their interaction with platelets play a key role in the acceleration of $FeCl_3$-induced thrombosis.

Key Words: Thrombosis, experimental animal models, red blood cells, platelet

INTRODUCTION

Among the in vivo thrombosis models, the ferric chloride ($FeCl_3$) model has been widely used for its simplicity, effectiveness, and reliability.[1] This model can be easily applied to a variety of vessels of different diameters, and it also displays a high degree of reproducibility and sensitivity to both anticoagulants and antiplatelet.[2] In this model, the application of $FeCl_3$ to the surface

Received: June 9, 2021 **Revised:** August 6, 2021 **Accepted:** August 19, 2021
Corresponding author: Ji Hoe Heo, MD, PhD, Department of Neurology, Yonsei University College of Medicine, Severance Integrative Research Institute for Cerebral and Cardiovascular Diseases, 50-1 Yonsei-ro, Seodaemoon-gu, Seoul 03722, Korea.
Tel: 82-2-2228-1605, Fax: 82-2-393-0705, E-mail: jhheo@yuhs.ac

•The authors have no potential conflicts of interest to disclose.

of a vessel induces thrombosis. Despite previous efforts to characterize the model, it still lacks standardization.[1,3] A wide range of $FeCl_3$ concentrations (2.5%–80%) have been reported for use in various strains of mice or rats.[4-8] However, limited information is available on the concentration-dependent effects on and sex-based differences in thrombus formation and stability.[9] Methodological differences in the $FeCl_3$-induced thrombosis model may significantly affect experimental results.[10] Moreover, they complicate inter-study comparisons and challenge researchers in determining the optimal conditions for their research.

Several mechanisms of $FeCl_3$-induced thrombosis have been suggested, including oxidative stress–induced vascular injury and red blood cell (RBC)-mediated platelet recruitment.[11-14] However, the exact mechanisms of $FeCl_3$-induced thrombosis remain uncertain.[15] Knowledge of the thrombus composition is important as it represents the primary thrombus characteristics and may reflect some aspects of the thrombosis mechanism. Although several studies have reported the presence of platelets, RBCs, and fibrin in $FeCl_3$-induced thrombi, limited information is available about the composition of each component.[16] Moreover, whether the composition differs according to $FeCl_3$ concentration remains unknown.

Therefore, despite the wide use of the $FeCl_3$-induced thrombosis model, several issues are still uncertain. In this study, using the carotid artery thrombosis model, we examined the effects of various $FeCl_3$ concentrations on the formation and stability of thrombi in two different strains of mice. We also showed the ultrastructural features of thrombi with some speculation on the mechanism of $FeCl_3$-induced thrombosis.

MATERIALS AND METHODS

Animals

All animal procedures were approved by the Institutional Animal Care and Use Committee of Yonsei University College of Medicine and performed in accordance with the Association for Assessment and Accreditation of Laboratory Animal Care (2018-0331). Seven- to 9-week-old mice from the Institute of Cancer Research (ICR) (male 32–34 g, female 27–29 g) and C57BL/6N mice (male 20–22 g, female 18–20 g) were purchased from Orient Bio Inc. (Seongnam, South Korea) to be used in the study.

Study design

First, to compare the effects of different concentrations of $FeCl_3$ on thrombus formation in the two different mouse strains, the time to occlusion and thrombus area were determined, and the thrombus composition was evaluated. Then, the effects of different concentrations of $FeCl_3$ on thrombus stability were compared. The ultrastructural morphology of the thrombi was examined by transmission electron microscopy (TEM) in ICR mice treated with 10% and 50% $FeCl_3$.

$FeCl_3$-induced arterial thrombosis model

The animals were anesthetized with 5% isoflurane in a mixture of 70% nitrous oxide and 30% oxygen; anesthesia was maintained with 2% isoflurane during the operative procedure. Body temperature was monitored and maintained at 37.0°C±0.2°C using a homoeothermic blanket control unit and a heating pad (Harvard Apparatus, Holliston, MA, USA). A midline cervical incision was made, and the left common carotid artery (CCA) was isolated under a surgical microscope. Carotid blood flow was monitored using an ultrasonic Doppler flow probe (MA0.7PSB; Transonic Instruments, Ithaca, NY, USA) connected to a Transonic TS420 blood flow meter (Transonic Instruments) and an iWorx IX-304T data acquisition system (iWorx Systems, Inc., Dover, NH, USA). Baseline flow was recorded for 5 min before the $FeCl_3$ treatment. Vascular injury was induced on the CCA by placing a filter paper (1×0.5 mm) saturated with different concentrations [10%, 20%, 30%, 40%, and 50% (w/v)] of $FeCl_3$ (F2877; Sigma-Aldrich Inc., St. Louis, MO, USA) for 5 min. The CCA was washed and excised at the end of the flow recording for 25 min after the $FeCl_3$ treatment.

Determination of time to and duration of occlusion

Time to occlusion was defined as the time from $FeCl_3$ application to the ceased blood flow (0 mL/min). The duration of occlusion was defined as the time from the initial occlusion to flow increase to 10% of the baseline flow. Recanalization was defined as the restoration of blood flow back to at least 50% of the baseline level.

Measurement of thrombus size

The excised CCA was fixed in 4% paraformaldehyde and embedded in paraffin. CCA paraffin blocks were sectioned longitudinally into 4-μm slices and stained with hematoxylin and eosin. The thrombus area was measured in the slide representing the largest part of the thrombus under a light microscope (Zeiss Imager D2, Carl Zeiss Imaging Solution, Oberkochen, Germany) and Zeiss AxioVision software (AxioVs40 V 4.8.1.0; Carl Zeiss Imaging Solution) using Image J software.

Immunohistochemistry of thrombus

Sectioned slices were deparaffinized and subjected to heat-induced epitope retrieval with retrieval solution (IHC World, Inc., MD, USA). After blocking with 5% horse serum, the sections were incubated with primary antibodies against fibrinogen/fibrin (ab34269; Abcam, Cambridge, UK), CD41 (ab63983; Abcam) for platelets, TER119 (BL116202; Biolegend, San Diego, CA, USA) for RBCs, Ly6G (BL127602; Biolegend) for neutrophils, and coagulation factor XIIIa (FXIIIa, PA5-22110; Invitrogen, Carlsbad, CA, USA). Endogenous peroxidase activity was blocked using 0.03% hydrogen peroxide. The sections were incubated for 30 min with 1:200-diluted biotin-conjugated secondary antibodies [goat anti-rabbit immunoglobulin G (IgG) antibody, BA-1000, and goat anti-rabbit IgG antibody, BA-9401; Vector Laboratories,

Burlingame, CA, USA] and then with horseradish peroxidase–conjugated streptavidin-biotin complex (ABC Elite Kit; Vector Laboratories). After counterstaining with hematoxylin, the colors were developed using NovaRed (NovaRed Kit; Vector Laboratories).

Measurement of thrombus composition

Thrombus composition was measured as previously described.[17] Briefly, images of immunostained thrombi were captured using a Zeiss light microscope and AxioVision software and processed using Image J software. After manual drawing of the thrombus contour, imaging analysis was performed semi-automatically using the color devolution module for Nova Red in Image J. Pixel density was determined using the auto threshold. The fraction (%) of each component (platelet, RBC, and fibrin) was calculated as the pixel density percentage for the entire thrombus. For neutrophils, Ly6G-positive cells were manually counted in the entire thrombus area using a motorized stage mounted on the microscope.

Assessment of thrombus stability

Blood flow was measured for 2 h. All measurements were standardized by subtracting the minimum blood flow. Blood flow restoration for 2 h was calculated by dividing the average blood flow by baseline flow and represented as a percentage.

Transmission electron microscopy

The excised arteries containing thrombi of ICR mice were immediately fixed with 2% glutaraldehyde and 2% paraformaldehyde in 0.1 M phosphate buffer (pH 7.4) overnight. The thrombi were post-fixed using 1% OsO_4 for 2 h. The thrombi were dehydrated, treated with propylene oxide for 10 min, and incubated overnight to allow penetration. The thrombi were then embedded using a Poly/Bed 812 Kit (Polysciences, Bergstrasse, Germany) and subjected to thermal polymerization in an electron microscope oven (TD-70; DOSAKA, Kyoto, Japan) for 12 h. The thrombi were sectioned at 200-nm slices and stained with toluidine blue. Areas of observation were selected, sectioned into 80 sections, and double-stained with 3% uranyl acetate for 30 min and 3% lead citrate for 7 min. The sections were imaged using a TEM (JEM-1011; JEOL, Tokyo, Japan) equipped with a Megaview III CCD camera (Soft Imaging System, Muenster, Germany).

Fibrin zymography

Blood samples were drawn into citrate tubes via cardiac puncture 30 min after the $FeCl_3$ treatment from five mice, each of the ICR and C57BL/6N mice with sham surgery, 10% $FeCl_3$ treatment, or 50% $FeCl_3$ treatment. The plasma was isolated by centrifuging the blood at 1000 g for 15 min in a refrigerated centrifuge and stored at -80°C until use. Sodium dodecyl sulfate–polyacrylamide gel electrophoresis was performed using 10% gels containing 0.075% fibrinogen (bovine; Sigma-Aldrich Inc.) and 1 NIH unit/mL of thrombin (human; Sigma-Aldrich Inc.).

Each plasma sample containing 50 μg of protein was loaded and electrophoresed under non-reducing conditions. In each gel, 3 ng of recombinant tissue plasminogen activator was loaded as an internal standard. The gels were rinsed with 2.5% Triton X-100 and incubated with reaction buffer (30 mM Tris, pH 7.4, 200 mM NaCl, and 0.02% NaN_3) for 24 h at 37°C. The gels were stained with 0.1% Amido black for 30 min and de-stained with methanol and acetic acid. The gels were scanned using a flatbed scanner (Epson Perfection V800 Photo; Seiko Epson Co., Nagano, Japan) and analyzed by ImageJ software.

Statistical analyses

Statistical analyses were performed using IBM SPSS statistics for Windows, version 25.0 (IBM Corp., Armonk, NY, USA). Three- or two-way analysis of variance (ANOVA) was performed for multiple analyses involving concentration, sex, and strain, followed by the post-hoc Bonferroni method. For trend analyses, ANOVA *p* values for trend tests were calculated using the general linear mode. Correlation analysis was performed using Pearson's correlation coefficient. Values are presented as mean± standard deviation. *p* values <0.05 were considered significant.

RESULTS

Thrombus formation by $FeCl_3$ concentration and mouse strain

A total of 50 ICR mice and 50 C57BL/6N mice were used to determine the time to occlusion according to the various concentrations of $FeCl_3$ (10%, 20%, 30%, 40%, and 50%, w/v) (five male and five female mice at each $FeCl_3$ concentration). In both ICR and C57BL/6N mice, higher concentrations of $FeCl_3$ induced a faster thrombotic occlusion. Although the time to occlusion was shortened in a dose-dependent manner in both ICR and C57BL/6N mice (*p* for trend <0.001 for both strains), the dose-dependency tended to be dampened from 30% to 50% in C57BL/6N mice (Fig. 1A). A significant interaction was observed between concentration and strain (F=2.784, *p*=0.032). No difference in time to occlusion was found between male and female mice (*p*=0.975) (Supplementary Tables 1 and 2, only online).

Higher concentrations of $FeCl_3$ produced larger thrombi in both ICR and C57BL/6N mice (Fig. 1B and Supplementary Table 3, only online). Thrombus size (area) increased in a dose-dependent manner in ICR mice (*p* for trend <0.020), but not in C57BL/6N mice (*p* for trend=0.111).

Changes of thrombus composition by $FeCl_3$ concentration

In the present study, topical application of $FeCl_3$-soaked filter paper on mouse carotid artery induced thrombus formation via the diffusion of $FeCl_3$ through the vessel wall (Fig. 2A). We evaluated the distribution of each thrombus component in the

https://doi.org/10.3349/ymj.2021.62.11.1032

resulting thrombi (Fig. 2B). Fibrin and platelet counts were evenly distributed throughout the thrombus. RBCs were seen as small clusters across the thrombus and predominantly accumulated near the regions of vascular injury induced by the $FeCl_3$ treatment. Neutrophils were mostly located in the periphery of the thrombus.

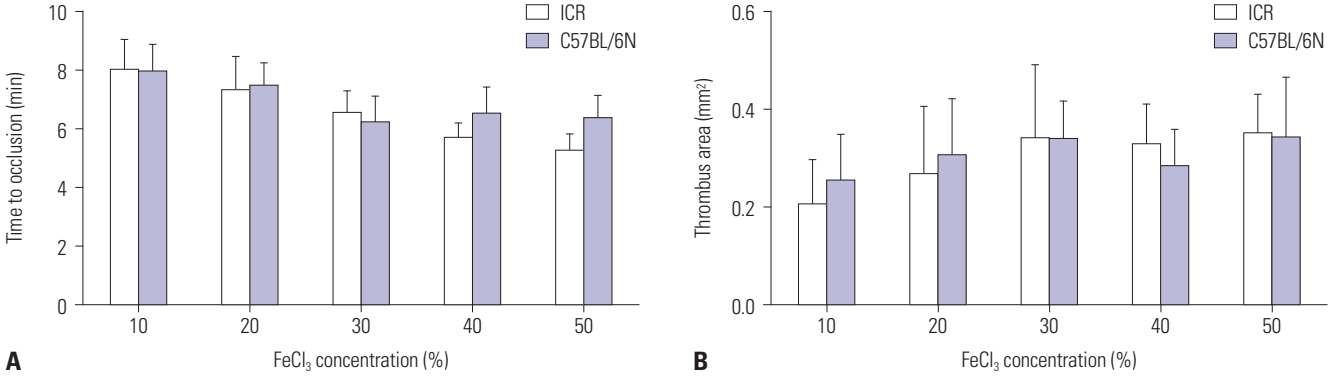

Fig. 1. Time to occlusion and thrombus area by different $FeCl_3$ concentrations. (A) Overall time to occlusion was shortened in a dose-dependent manner in ICR mice and C57BL/6N mice. However, it tended to be dampened from 30% to 50% in C57BL/6N mice. (B) Thrombus size (area) increased in a dose-dependent manner in ICR mouse but not in C57BL/6N mice (p for trend=0.020 for ICR, p for trend=0.111 for C57BL/6N). Bars represent the mean±standard deviation. Ten mice (five male, five female) of each strain were used at each concentration. ICR, Institute of Cancer Research.

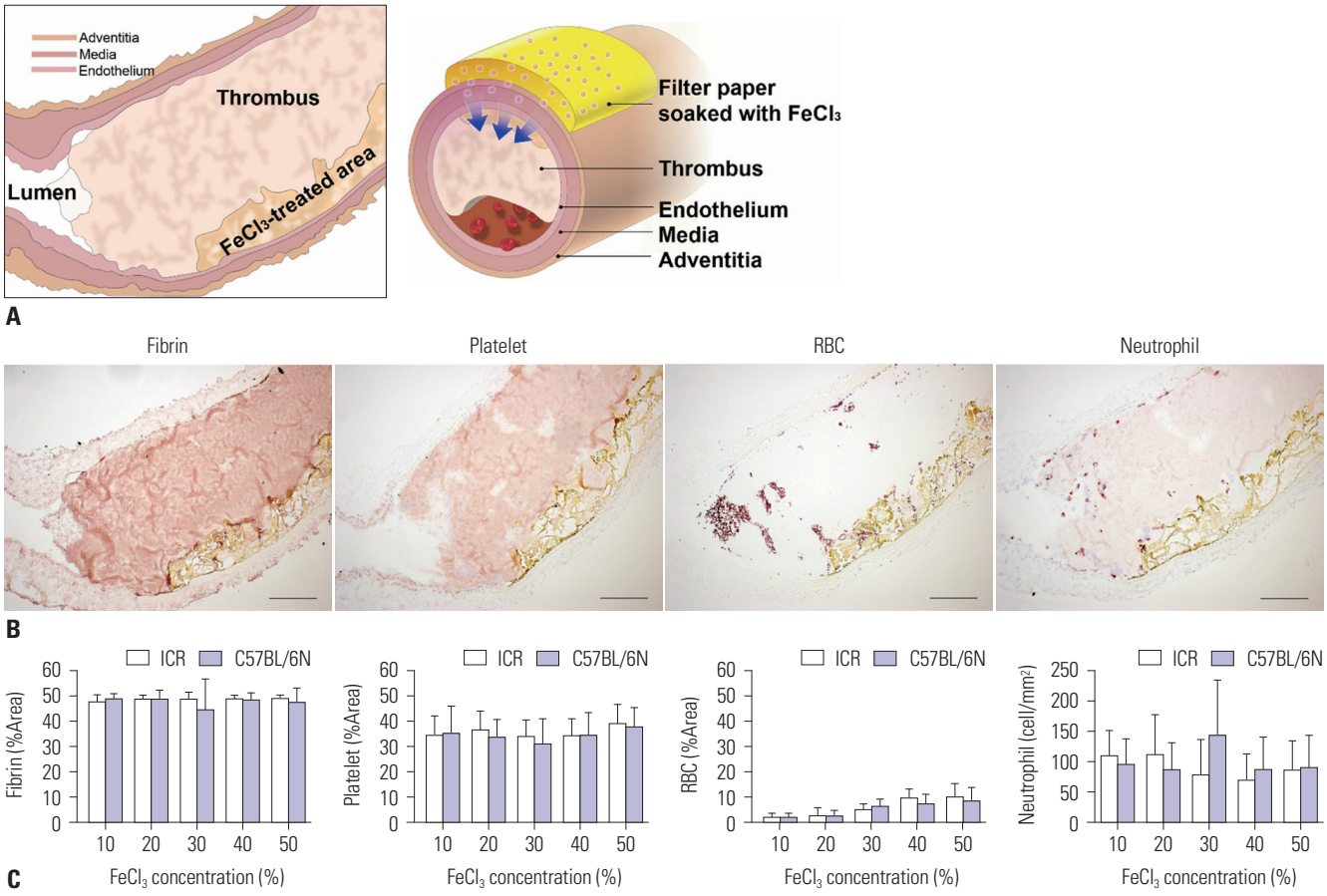

Fig. 2. Composition of $FeCl_3$-induced mouse carotid artery thrombi at various $FeCl_3$ treatment concentrations. (A) Tracings of the representative thrombus in the cross-section of mouse carotid artery (left) and schematic of thrombus formation by $FeCl_3$ (right). (B) Representative immunohistochemistry of fibrin, platelet, RBCs, and neutrophils in mouse thrombus. Fibrin and platelets are evenly distributed. However, many RBCs are seen as clusters or near the $FeCl_3$-treated area. Neutrophils are located at the periphery of the thrombus. Immunoreactivity is shown as red (NovaRed stain). Scale bar=100 μm. (C) Comparison of thrombus composition at various $FeCl_3$ concentrations for the two mouse strains. %Areas for fibrin, platelets, and RBCs are shown, while cells/mm^2 are shown for neutrophils. RBC content increased with increasing $FeCl_3$ concentrations (p for trend <0.001 for ICR mice and C57BL/6N mice). Ten mice (five male, five female) were used of each strain at each concentration. Bars represent means±standard deviation. ICR, Institute of Cancer Research; RBCs, red blood cells.

We investigated whether the concentration of $FeCl_3$ affected the histological composition of the thrombus. As the concentration of $FeCl_3$ increased, RBC content increased in both mouse strains (p for trend <0.001 for both strains) (Figs. 2C and 3). Other components (fibrin, platelets, and neutrophils) did not change with different $FeCl_3$ concentrations (Fig. 2C). There were no sex-based differences in the thrombus composition (Supplementary Tables 4 and 5, only online).

Association between RBC content and time to occlusion and thrombus size

Since the $FeCl_3$ concentration was associated with time to occlusion and RBC content, we investigated whether the RBC content in the thrombus correlates with time to occlusion. There was an inverse correlation between time to occlusion and RBC content in the entire mouse population (r=-0.65, p<0.001) (Fig. 4A). An inverse correlation was observed in ICR mice (male, r=-0.75, p<0.001; female, r=-0.83, p<0.001) and C57BL/6N mice (male, r=-0.63, p<0.001; female, r=-0.62, p<0.001) (Supplementary Fig. 1, only online). There was no significant difference between the two strains (p=0.131). No significant association was observed between RBC content and thrombus size (r=0.19, p<0.059) (Fig. 4B).

Ultrastructural morphology of thrombus

The ultrastructure of the thrombus was examined using TEM. Mouse thrombi induced by 50% $FeCl_3$ showed increased RBC accumulation and larger RBC aggregates compared to those induced by 10% $FeCl_3$ (Fig. 5A and B). Polyhedrocytes and intermediate forms of RBCs were observed after 10% and 50% $FeCl_3$ treatment. RBCs were surrounded by closely attached platelets. RBCs were attached to and surrounded by aggregates of degranulated platelets. These features were observed in RBCs adjacent to the injured vessels as well as those in the middle of the thrombus (Fig. 5A-C). Platelets were aggregated and packed throughout the thrombus, and some were attached to the endothelium. Platelets adjacent to the $FeCl_3$-treated endothelium also showed degranulation, although to a lesser degree than those attached to RBCs (Fig. 5D). Fibrin fibers were interposed between RBCs and platelets. Degranulated platelets were more frequently noted in thrombi induced by 50% $FeCl_3$ than in those treated with 10% $FeCl_3$ (Fig. 5).

Thrombus stability according to $FeCl_3$ concentration and mouse strain

For this experiment, blood flow was monitored for 2 h after the $FeCl_3$-induced thrombosis. Only male mice were used, as there

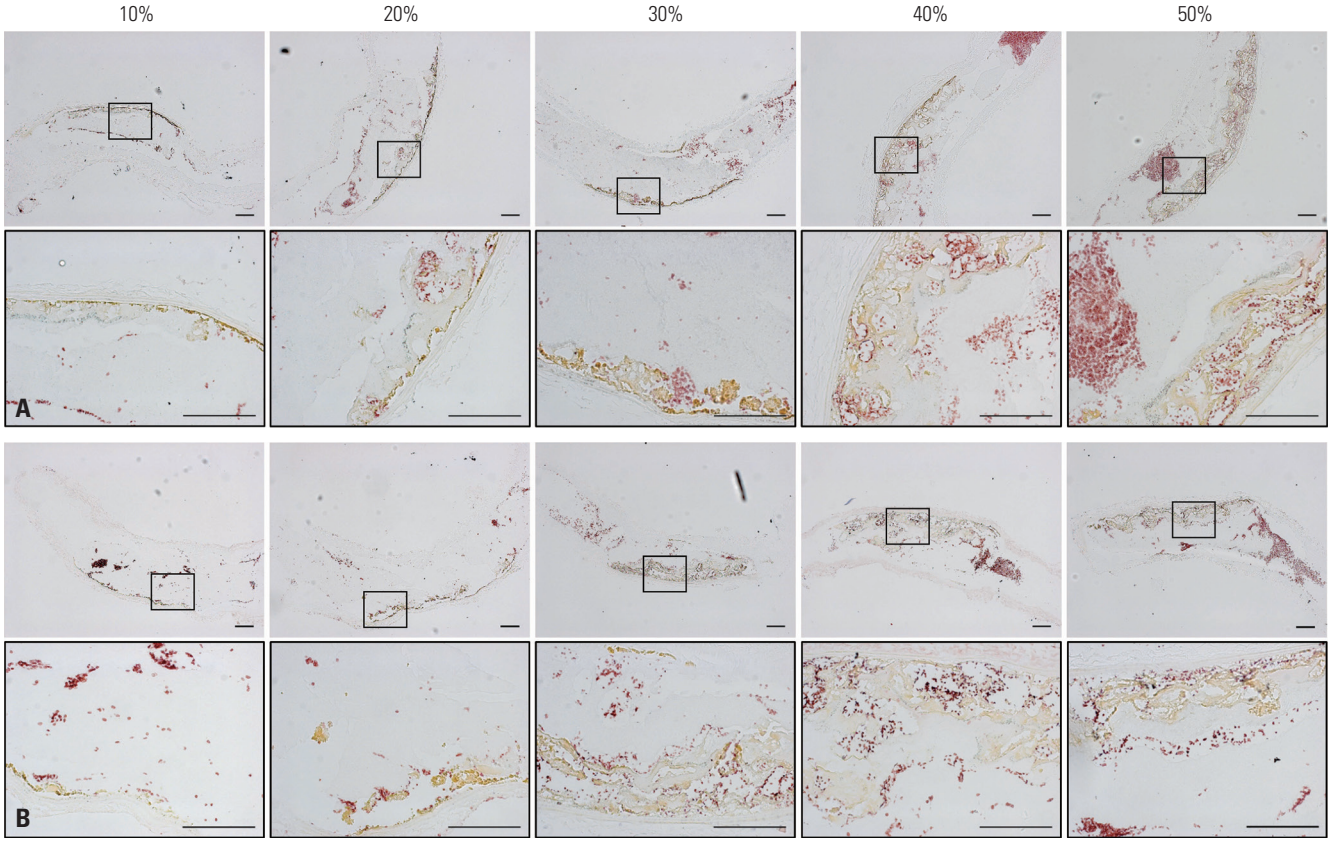

Fig. 3. Dose-dependent effect of $FeCl_3$ on RBC content. Representative images of cross-sectional mouse thrombi immunostained for RBCs in (A) ICR mice and (B) C57BL/6N mice. The numbers above images indicate the $FeCl_3$ concentrations used. As the $FeCl_3$ concentration increased, the RBC content increased in the thrombus and near the $FeCl_3$-treated area. The upper panel shows mice thrombus and the lower panel shows higher-magnification images of the regions of severe damage induced by $FeCl_3$. RBCs are shown in red (NovaRed staining). Scale bar=100 μm. ICR, Institute of Cancer Research; RBC, red blood cells.

https://doi.org/10.3349/ymj.2021.62.11.1032

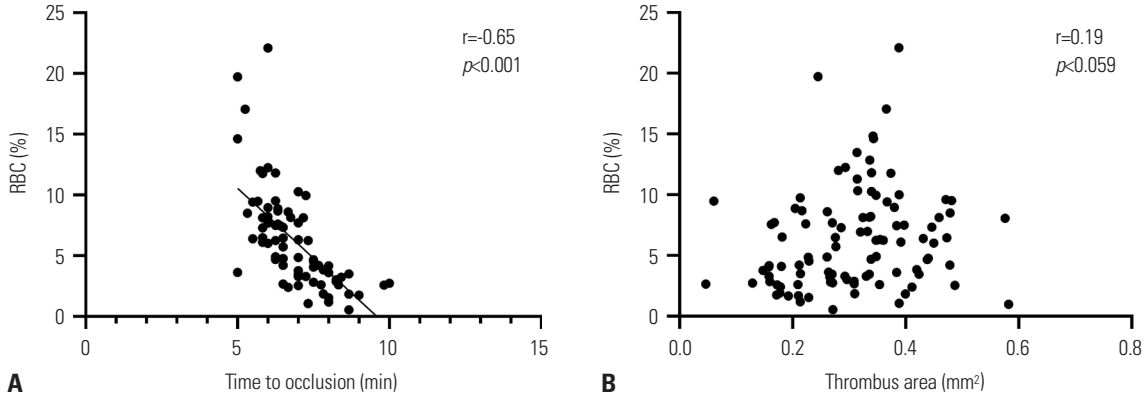

Fig. 4. Correlation of the amount of RBCs with time to occlusion and thrombus size in mice. (A) Time to occlusion negatively correlated with RBC content. (B) Thrombus size and RBC content did not show a significant relationship. Correlation analysis was performed using Pearson's correlation. Pearson's coefficient r and *p* values are presented. A total of 100 mice were included in the correlation analysis. RBC, red blood cell.

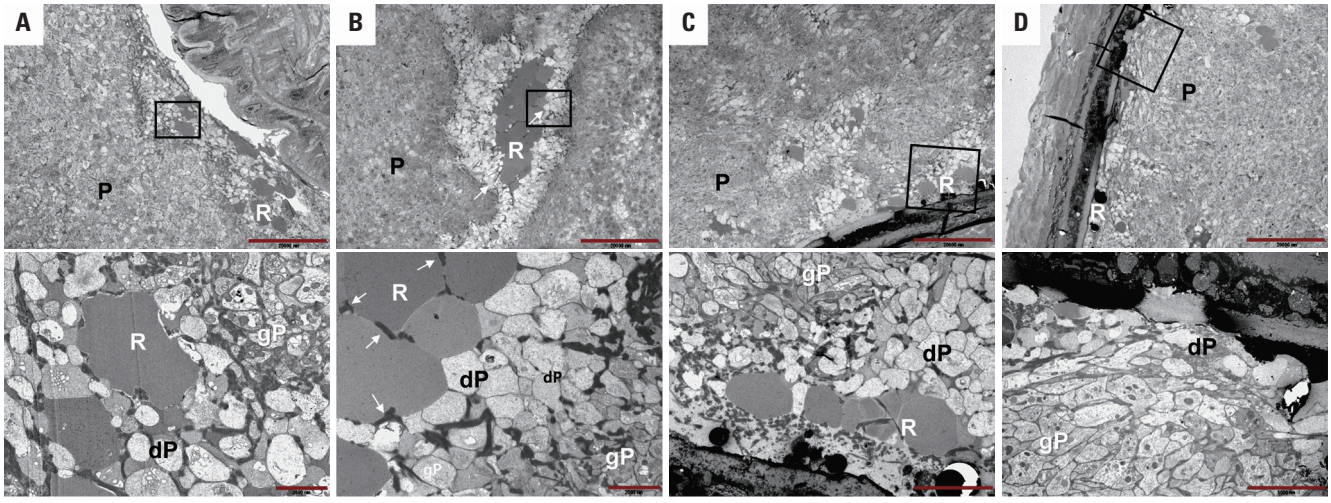

Fig. 5. Red blood cell aggregation and platelet degranulation in 10% and 50% $FeCl_3$-induced mouse thrombi. Representative transmission electron microscopic images of mouse thrombi induced by (A) 10% $FeCl_3$ and (B–D) 50% $FeCl_3$. The lower panel images are magnified views of the upper panel images. Red blood cells are surrounded by degranulated platelets in (A) and (B). Fibrin fibers are observed within the red blood cell aggregates (arrows). Images of the thrombus near the $FeCl_3$-treated endothelium (C and D). Many degranulated platelets are seen around the red blood cells attached to the endothelium (C). Degranulated platelets are attached to the $FeCl_3$-treated endothelium. Thrombi from three mice treated with 10% $FeCl_3$ and those from four mice treated with 50% $FeCl_3$ were observed. R, red blood cell; P, platelet; dP, granulated platelet; gP, granulated platelet. Upper panel: original magnification=×1500, scale bar=20000 nm, (A and B) lower panel: original magnification=×10000, scale bar=2000 nm, (C and D) lower panel: original magnification=×6000, scale bar=5000 nm.

were no sex-based differences in the time to occlusion results. For both mouse strains, the mean blood flow for 2 h of recording decreased with higher $FeCl_3$ concentrations (p for trend=0.005 for ICR, p for trend=0.001 for C57BL/6N) (Fig. 6A), suggesting that the thrombus was more frequently resolved at lower concentrations. However, the restoration of blood flow differed between ICR mice and C57BL/6N mice at lower (10% and 20%) $FeCl_3$ concentrations. The mean blood flow for 2 h was significantly lower in ICR mice than in C57BL/6N mice (21.9% vs. 71.2% in 10% $FeCl_3$, and 11.8% vs. 62% in 20% $FeCl_3$, $p<0.050$), which suggests that thrombus resolution at lower concentrations occurs more frequently in C57BL/6N mice than in ICR mice. The duration of occlusion was prolonged at higher concentrations (p for trend <0.001 for ICR, p for trend=0.002 for C57BL/6N) (Fig. 6B). At every $FeCl_3$ concentration, at least one of five C57BL/6N mice had recanalization during 2 h of monitoring, and all C57BL6 mice treated with 10% $FeCl_3$ showed recanalization. However, among ICR mice, none showed recanalization after 40% or 50% $FeCl_3$ treatment (Table 1).

We further examined whether spontaneous recanalization at lower $FeCl_3$ concentrations and the difference between mouse strains were associated with endogenous fibrinolysis or fibrin retraction. In fibrin zymography, there were no differences in the fibrinolytic activities of tissue-type plasminogen activator and urokinase-type plasminogen activator between ICR and C57BL/6N mice (p=0.321) or between 10% and 50% $FeCl_3$ concentrations (p=0.988) (Fig. 6C and E). However, the optical density of FXIIIa in thrombus, which plays a role in thrombus (fibrin) stability, was significantly lower in C57BL/6N mice than in ICR mice ($p<0.001$) (Fig. 6D and F).

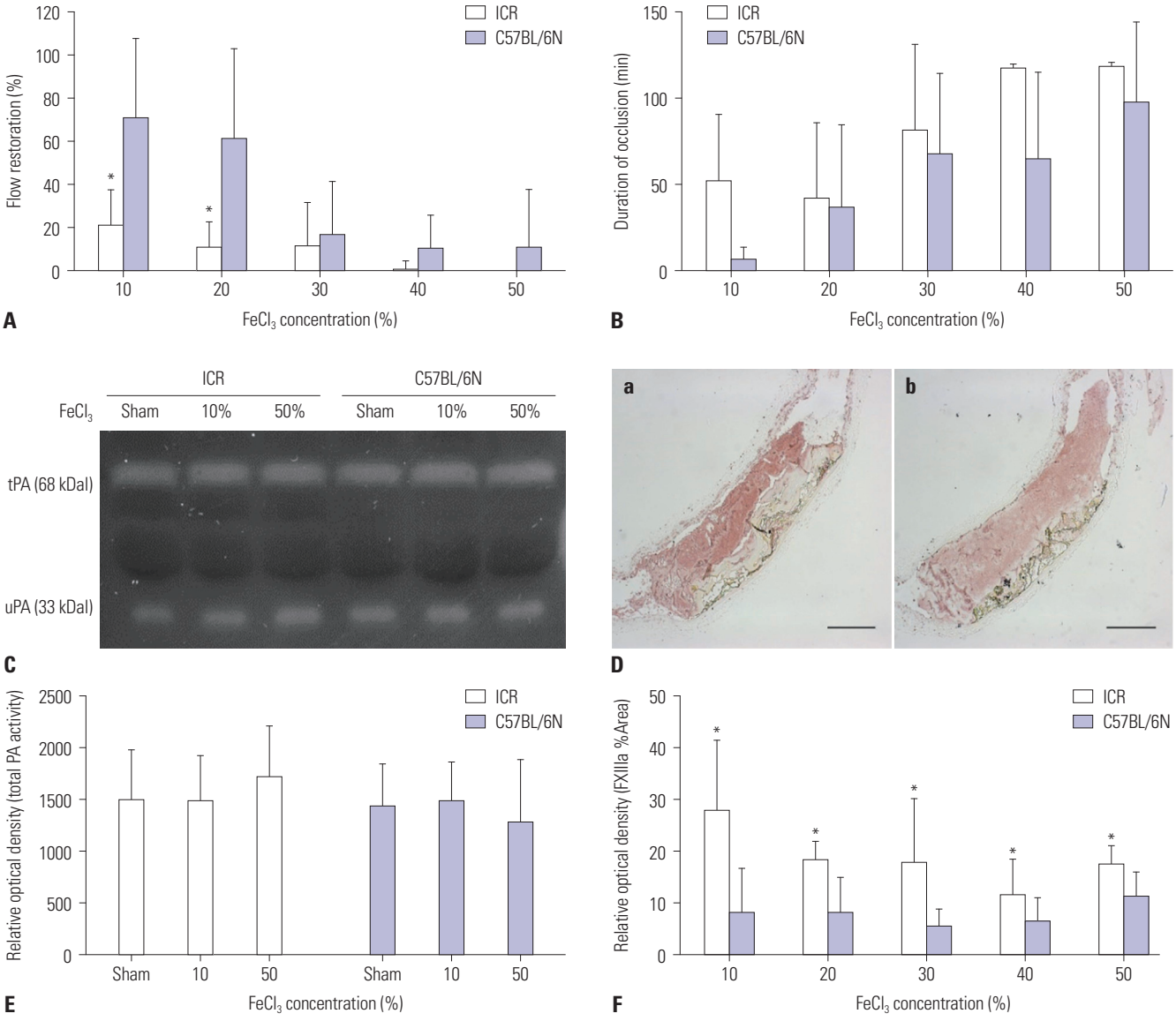

Fig. 6. Evaluation of thrombus stability and stability-related factors by $FeCl_3$ concentration and mouse strain. Blood flow of the occluded carotid arteries was recorded for 2 h. Five male mice of each strain were used at each concentration. (A) Flow restoration decreased dose-dependently in both ICR and C57BL/6N mice (p for trend=0.005, p for trend=0.001, respectively). At 10%–20%, ICR mice showed significantly lower blood flow restoration. (B) Duration of occlusion increased dose-dependently in both ICR and C57BL/6N mice (p for trend <0.001, p for trend=0.002, respectively). Overall, more stable thrombi were produced in ICR mice compared to C57BL/6N mice. (C) Fibrin zymography analysis showing fibrinolytic activities of plasminogen activators in the plasma of mice with either sham surgery, 10% $FeCl_3$ treatment, or 50% treatment. (D) Representative images of immunohistochemistry against FXIIIa in thrombi from (a) ICR mice and (b) C57BL/6N mice. Scale bar=200 μm. (E) The relative optical density of plasminogen activator activity was not different across all concentrations or mouse strains. (F) The relative intensity of FXIIIa was significantly higher in ICR mice at all $FeCl_3$ concentrations. Bars represent mean±standard deviation. *p<0.050 versus C57BL/6N. Five male mice of each strain were used at each concentration. ICR, Institute of Cancer Research.

DISCUSSION

This study demonstrated that $FeCl_3$ has dose-dependent effects on arterial thrombosis. The time to occlusion was shortened with increasing $FeCl_3$ concentration from 10% to 50%. Moreover, thrombus size increased with increasing $FeCl_3$ concentration. Previous studies using a fluorescent video microscope showed that higher $FeCl_3$ concentrations induced faster thrombus formation in the range of 2.5% to 20% of $FeCl_3$.[2,10] Findings in this study are consistent with those of previous studies and further demonstrated the dose-dependency at much higher $FeCl_3$ concentrations.

However, the reason why higher $FeCl_3$ concentrations accelerate thrombosis remains unknown. The thrombus composition may reflect some aspects of the thrombosis mechanism. This study showed that $FeCl_3$-induced thrombus is primarily fibrin- and platelet-rich, which suggests that platelets are engaged in $FeCl_3$-induced thrombosis. However, the compositions

https://doi.org/10.3349/ymj.2021.62.11.1032

Table 1. Recanalization Rate During 2 h of Monitoring after Occlusion

Mouse strain	Ferric chloride concentration				
	10% (n=5)	20% (n=5)	30% (n=5)	40% (n=5)	50% (n=5)
Institute of Cancer Research	3 (60)	2 (40)	2 (40)	0 (0)	0 (0)
C57BL/6N	5 (100)	4 (80)	1 (20)	1 (20)	1 (20)

Values in parentheses are percentages. Recanalization was defined as blood flow restored to at least 50% of the baseline level after occlusion.

of the platelets and fibrin were independent of $FeCl_3$ concentration. They were not localized to the area of $FeCl_3$ treatment but were more evenly distributed throughout the entire thrombus. In contrast, the proportion of RBCs increased with increasing $FeCl_3$ concentration, the amount of RBC was inversely correlated with time to occlusion, and RBCs were predominantly localized near $FeCl_3$ treatment area. These findings suggest that, while platelets are involved in $FeCl_3$-induced thrombosis, RBCs play an important role in the $FeCl_3$ concentration-dependent acceleration of thrombosis.

The exact mechanisms of thrombosis in the $FeCl_3$-induced model remain uncertain. $FeCl_3$-induced oxidative stress was suggested to result in vascular injury and lead to platelet adhesion to the injury site and subsequent aggregation of platelets with thrombus formation.[14] Recent studies suggested that RBCs may be the initial cells to participate in thrombosis by binding to the $FeCl_3$-treated endothelial surfaces.[11,12] The studies showed that, upon $FeCl_3$ treatment, RBCs adhered to Fe^{3+} ions via their physiochemical properties and formed initial aggregates by recruiting platelets.[11,12] Mice with a high hematocrit exhibited a faster time to artery occlusion in the $FeCl_3$ model.[18] In a previous study using a microfluidic device designed to replicate the endothelium-blood environment, the flocculation activity of $FeCl_3$ increased with increasing $FeCl_3$ concentrations, aggregating RBCs and other blood components.[12] Those findings, along with ours, suggest that RBCs and platelets play an important role in $FeCl_3$-induced thrombosis.

Furthermore, we found that platelets attached or adjacent to RBCs were extensively degranulated. Platelets have dense granules containing countless small molecules.[19,20] These granules are released upon platelet activation and recruit more platelets to the vessel injury.[19] Previous studies demonstrated that RBCs activate adjacent platelets by releasing substances such as ADP and thromboxane A_2.[21,22] Our findings indicate that platelets adjacent to RBCs extensively release granules immediately after $FeCl_3$ treatment. The released platelet granules may contribute to the activation, aggregation, and further recruitment of platelets.

However, it is unknown how $FeCl_3$ affects RBCs and how RBCs interact with platelets. $FeCl_3$ may generate free radicals, and exposure of RBCs to $FeCl_3$ is known to result in lipid peroxidation.[14] In this study, $FeCl_3$ rendered RBC morphological changes in polyhedrocytic or intermediate forms. RBC fragmentation was seen in the $FeCl_3$ model.[11] Oxidative stress induced by $FeCl_3$ treatment might be associated with the changes in RBC morphology.[23] Phosphatidylserine is exposed when cells are damaged by oxidative stress or shear stress.[22,24,25] Externalization of phosphatidylserine on RBC membranes generates thrombin burst.[21] Thrombin produces fibrin and further activates platelets. The presence of fibrin fibers between RBC aggregates on TEM in this study suggests that thrombin might play a role in fibrin production. These findings suggest that the damage to RBCs induced by $FeCl_3$ might contribute to thrombosis by platelet activation and thrombin generation.

However, in this study, RBCs comprised only about 10% of the thrombi. Additionally, degranulation of some platelets in the absence of RBCs was also observed near the $FeCl_3$-treated endothelium, implying that $FeCl_3$ might also affect platelets. The externalization of phosphatidylserine on activated platelets is also known to possess hypercoagulability.[26,27] These findings suggest that $FeCl_3$ may affect various cells in the blood and mediate thrombosis via more diverse and complex mechanisms.

Most previous studies on $FeCl_3$-induced thrombosis focused on the initial stage of thrombosis and measured the time to occlusion to determine effective thrombosis. The stability of a thrombus induced by $FeCl_3$ is less well known. In this study, the stability of the thrombus differed by $FeCl_3$ concentration and mouse strain. In both ICR and C57BL/6N mice, higher $FeCl_3$ induced the formation of a more stable thrombus in a dose-dependent manner. However, we found that ICR and C57BL/6N mice showed different thrombus stabilities, especially at lower concentrations of $FeCl_3$. ICR mice produced more stable thrombi with less variation than C57BL/6N mice. This information on thrombus stability may be helpful for designing mechanistic studies that require stable clots and evaluating the efficacy of thrombolytic drugs.

Resolution of the thrombus that formed after $FeCl_3$ treatment might be related to spontaneous fibrinolysis or insufficient clot contraction. We evaluated the key mediators of these processes, which include fibrinolytic activity by plasminogen activators and fibrin stability by FXIIIa. In this study, fibrinolytic activities did not differ by $FeCl_3$ concentration or mouse strain. However, the immunoreactivity of FXIIIa was higher in ICR mouse thrombi than in C57BL/6N mouse thrombi. FXIIIa catalyzes the cross-linking of fibrin fibers, contributing to enhanced thrombus stability and resistance to thrombolysis.[28-31] The less stable thrombus in C57BL/6N mice may be partly explained by the lower levels of FXIIIa in their thrombi.

This study had some limitations. Although we visualized direct evidence of platelet activation in relation to RBCs by showing the degranulation of platelets adjacent to them, the mechanism of RBC–platelet interaction by $FeCl_3$ remains unknown. Also, the response to $FeCl_3$ may differ according to filter paper size and exposure duration. Furthermore, although we investigated the role of RBC in the $FeCl_3$ model, the contribution of neutrophils, which have an emerging role in arterial thrombosis, was not evaluated in this study. Neutrophils, which are known to accumulate with thrombus age,[32] may be better studied in

thrombi that are more aged than the very fresh thrombi analyzed in this study. Lastly, as we tested two mouse strains, the responses to $FeCl_3$ in other mouse strains and other species are unknown.

Nonetheless, our findings provide evidence of RBC-associated thrombosis acceleration and platelet activation to the recent notion that emphasizes the active role of RBCs in thrombosis.[23] Our results provide some insight into optimizing experiments using $FeCl_3$. $FeCl_3$ did not significantly alter thrombus composition across all concentrations (10%–50%), except for RBCs. Furthermore, all animals had occlusions within these concentration ranges. Thus, any $FeCl_3$ concentration tested in our study may be used to evaluate thrombus formation. However, in cases requiring stable thrombus, including mechanistic studies using aged thrombi and evaluating thrombolytic agents, higher concentrations are needed. Of the two mouse strains tested in this study, ICR mice were more reliable than C57BL/6N mice in terms of better dose-dependency and thrombus stability.

In conclusion, we showed that the $FeCl_3$ model produces thrombi rich in fibrin and platelets. The visualization of possible RBC–platelet interactions in mouse thrombi may help expand our understanding on the mechanisms of $FeCl_3$-induced thrombosis. The $FeCl_3$ model showed different responses in thrombus formation and stability according to $FeCl_3$ concentration and mouse strain. These findings may help researchers plan future experiments using the $FeCl_3$ model.

ACKNOWLEDGEMENTS

This study was supported by the Basic Science Research Program through the National Research Foundation of Korea (NRF), funded by the Ministry of Education (NRF-2018R1A2A3074996 and 2021R1A2C2003658), and by a faculty research grant of Yonsei University College of Medicine (6-2020-0202).

The authors would like to thank biostatistician Yun Ho Rho, MS (Department of Biomedical Systems Informatics, Yonsei University College of Medicine) for the statistical assistance, as well as the Medical Illustration & Design (part of Medical Research Support Services of Yonsei University College of Medicine) for all of the artistic support related to this work.

AUTHOR CONTRIBUTIONS

Conceptualization: Ji Hoe Heo and Il Kwon. Data curation: Yeseul Shim, Youngseon Park, and Jayoung Kim. Formal analysis: Il Kwon and Yeseul Shim. Funding acquisition: Ji Hoe Heo. Investigation: Yeseul Shim. Methodology: Il Kwon and Yeseul Shim. Project administration: Ji Hoe Heo, Young Dae Kim, Hyo Suk Nam, and Sungha Park. Resources: all authors. Software: all authors. Supervision: Ji Hoe Heo. Validation: Ji Hoe Heo, Il Kwon, and Heow Won Lee. Visualization: Ji Hoe Heo and Yeseul Shim. Writing—original draft: Yeseul Shim. Writing—review & editing: Ji Hoe Heo. Approval of final manuscript: all authors.

ORCID iDs

Yeseul Shim https://orcid.org/0000-0002-5618-8044
Il Kwon https://orcid.org/0000-0001-9449-5646
Youngseon Park https://orcid.org/0000-0001-7723-7194
Heow Won Lee https://orcid.org/0000-0003-3733-4453
Jayoung Kim https://orcid.org/0000-0003-0213-3512
Young Dae Kim https://orcid.org/0000-0001-5750-2616
Hyo Suk Nam https://orcid.org/0000-0002-4415-3995
Sungha Park https://orcid.org/0000-0001-5362-478X
Ji Hoe Heo https://orcid.org/0000-0001-9898-3321

REFERENCES

1. Bonnard T, Hagemeyer CE. Ferric chloride-induced thrombosis mouse model on carotid artery and mesentery vessel. J Vis Exp 2015:e52838.
2. Li W, McIntyre TM, Silverstein RL. Ferric chloride-induced murine carotid arterial injury: a model of redox pathology. Redox Biol 2013;1:50-5.
3. Li W, Nieman M, Sen Gupta A. Ferric chloride-induced murine thrombosis models. J Vis Exp 2016:54479.
4. Konstantinides S, Schäfer K, Thinnes T, Loskutoff DJ. Plasminogen activator inhibitor-1 and its cofactor vitronectin stabilize arterial thrombi after vascular injury in mice. Circulation 2001;103:576-83.
5. Kwon I, Hong SY, Kim YD, Nam HS, Kang S, Yang SH, et al. Thrombolytic effects of the snake venom disintegrin saxatilin determined by novel assessment methods: a FeCl3-induced thrombosis model in mice. PLoS One 2013;8:e81165.
6. Marx I, Christophe OD, Lenting PJ, Rupin A, Vallez MO, Verbeuren TJ, et al. Altered thrombus formation in von Willebrand factor–deficient mice expressing von Willebrand factor variants with defective binding to collagen or GPIIbIIIa. Blood 2008;112:603-9.
7. Wang X, Xu L. An optimized murine model of ferric chloride-induced arterial thrombosis for thrombosis research. Thromb Res 2005;115:95-100.
8. Zhang Y, Li L, Zhao Y, Han H, Hu Y, Liang D, et al. The myosin II inhibitor, blebbistatin, ameliorates FeCl3-induced arterial thrombosis via the GSK3β-NF-κB pathway. Int J Biol Sci 2017;13:630-9.
9. Polak D, Talar M, Watala C, Przygodzki T. Intravital assessment of blood platelet function. A review of the methodological approaches with examples of studies of selected aspects of blood platelet function. Int J Mol Sci 2020;21:8334.
10. Eckly A, Hechler B, Freund M, Zerr M, Cazenave JP, Lanza F, et al. Mechanisms underlying FeCl3-induced arterial thrombosis. J Thromb Haemost 2011;9:779-89.
11. Barr JD, Chauhan AK, Schaeffer GV, Hansen JK, Motto DG. Red blood cells mediate the onset of thrombosis in the ferric chloride murine model. Blood 2013;121:3733-41.
12. Ciciliano JC, Sakurai Y, Myers DR, Fay ME, Hechler B, Meeks S, et al. Resolving the multifaceted mechanisms of the ferric chloride thrombosis model using an interdisciplinary microfluidic approach. Blood 2015;126:817-24.
13. Neeves KB. Physiochemical artifacts in FeCl3 thrombosis models. Blood 2015;126:700-1.
14. Woollard KJ, Sturgeon S, Chin-Dusting JP, Salem HH, Jackson SP. Erythrocyte hemolysis and hemoglobin oxidation promote ferric chloride-induced vascular injury. J Biol Chem 2009;284:13110-8.
15. Schoenwaelder SM, Jackson SP. Ferric chloride thrombosis model: unraveling the vascular effects of a highly corrosive oxidant. Blood 2015;126:2652-3.

16. Wang L, Miller C, Swarthout RF, Rao M, Mackman N, Taubman MB. Vascular smooth muscle-derived tissue factor is critical for arterial thrombosis after ferric chloride-induced injury. Blood 2009;113:705-13.
17. Park H, Kim J, Ha J, Hwang IG, Song TJ, Yoo J, et al. Histological features of intracranial thrombi in stroke patients with cancer. Ann Neurol 2019;86:143-9.
18. Walton BL, Lehmann M, Skorczewski T, Holle LA, Beckman JD, Cribb JA, et al. Elevated hematocrit enhances platelet accumulation following vascular injury. Blood 2017;129:2537-46.
19. Rendu F, Brohard-Bohn B. The platelet release reaction: granules' constituents, secretion and functions. Platelets 2001;12:261-73.
20. Whiteheart SW. Platelet granules: surprise packages. Blood 2011;118:1190-1.
21. Reimers RC, Sutera SP, Joist JH. Potentiation by red blood cells of shear-induced platelet aggregation: relative importance of chemical and physical mechanisms. Blood 1984;64:1200-6.
22. Weisel JW, Litvinov RI. Red blood cells: the forgotten player in hemostasis and thrombosis. J Thromb Haemost 2019;17:271-82.
23. Becatti M, Marcucci R, Gori AM, Mannini L, Grifoni E, Alessandrello Liotta A, et al. Erythrocyte oxidative stress is associated with cell deformability in patients with retinal vein occlusion. J Thromb Haemost 2016;14:2287-97.
24. Sener A, Ozsavci D, Bingol-Ozakpinar O, Cevik O, Yanikkaya-Demirel G, Yardimci T. Oxidized-LDL and Fe3+/ascorbic acid-induced oxidative modifications and phosphatidylserine exposure in human platelets are reduced by melatonin. Folia Biol (Praha) 2009;55:45-52.
25. Reddy EC, Rand ML. Procoagulant phosphatidylserine-exposing platelets in vitro and in vivo. Front Cardiovasc Med 2020;7:15.
26. Zhao L, Bi Y, Kou J, Shi J, Piao D. Phosphatidylserine exposing-platelets and microparticles promote procoagulant activity in colon cancer patients. J Exp Clin Cancer Res 2016;35:54.
27. Reddy EC, Wang H, Christensen H, McMillan-Ward E, Israels SJ, Bang KWA, et al. Analysis of procoagulant phosphatidylserine-exposing platelets by imaging flow cytometry. Res Pract Thromb Haemost 2018;2:736-50.
28. Byrnes JR, Wolberg AS. Newly-recognized roles of factor XIII in thrombosis. Semin Thromb Hemost 2016;42:445-54.
29. Gorog DA, Fayad ZA, Fuster V. Arterial thrombus stability: does it matter and can we detect it? J Am Coll Cardiol 2017;70:2036-47.
30. Leidy EM, Stern AM, Friedman PA, Bush LR. Enhanced thrombolysis by a factor XIIIa inhibitor in a rabbit model of femoral artery thrombosis. Thromb Res 1990;59:15-26.
31. Shebuski RJ, Sitko GR, Claremon DA, Baldwin JJ, Remy DC, Stern AM. Inhibition of factor XIIIa in a canine model of coronary thrombosis: effect on reperfusion and acute reocclusion after recombinant tissue-type plasminogen activator. Blood 1990;75:1455-9.
32. Novotny J, Chandraratne S, Weinberger T, Philippi V, Stark K, Ehrlich A, et al. Histological comparison of arterial thrombi in mice and men and the influence of Cl-amidine on thrombus formation. PLoS One 2018;13:e0190728.